2022 American Control Conference (ACC)
Atlanta, USA, June 8-10, 2022

Toward stochastic dynamical wake-modeling for wind farms

Aditya H. Bhatt and A. Zare

Abstract— **Low-fidelity analytical models of turbine wakes have traditionally been used to demonstrate the utility of advanced control algorithms in increasing the annual energy production of wind farms. In practice, however, it remains challenging to achieve significant performance improvements using closed-loop strategies that are based on conventional low-fidelity models. This is due to the over-simplified static nature of wake predictions from models that are agnostic to the complex aerodynamic interactions among turbines. To improve the predictive capability of low-fidelity models while remaining amenable to control design, we offer a stochastic dynamical modeling framework for capturing the effect of atmospheric turbulence on the thrust force and power generation as determined by the actuator disk concept. In this approach, we use stochastically forced linear models of the turbulent velocity field to augment the analytically computed wake velocity and achieve consistency with higher-fidelity models in capturing power and thrust force measurements. The power-spectral densities of our stochastic models are identified via convex optimization to ensure statistical consistency while preserving model parsimony.**

Index Terms— **Control-oriented modeling, convex optimization, state covariances, stochastically forced Navier-Stokes equations, wake modeling, turbulence modeling, wind energy.**

I. Introduction

Wind energy has been recognized as an important natural source of sustainable energy that can play a major role in mitigating the environmental impacts of the ever-growing global energy demand. With the exponential rise in wind energy production, scientific efforts are shifting toward gaining a better understanding of the physics of atmospheric flows and how tools from optimization and control can improve the efficiency of wind farms [1]. A major challenge in wind farm control arises from the importance of nonlinear aerodynamic interactions among turbines. Such interactions are caused by the operation of downwind turbines in the wakes of upwind ones [2] and result in a reduction in power production and an elevation in dynamic loads while inducing wake recovery. An accurate representation of wake turbulence can thus profoundly affect the performance of control strategies in improving energy production and structural durability.

Given the importance of capturing the complexities of the wake, closed-loop control design has relied on computationally expensive models such as those that are used in large-eddy simulations (LES) of wind farms, e.g., [3]–[5]. While such models play an important role in improving our understanding of wake turbulence, they are not suitable for the development of online model-based control strategies that can adapt to time-varying atmospheric conditions informed by supervisory control and data acquisition (SCADA) measurements. This motivates the development of lower fidelity models that capture the essential flow features and quantities of interest for analysis or control.

Seminal efforts in developing low-fidelity models of turbine wakes focused on two-dimensional (2D) heuristic-based methods that capture the steady-state velocity at hub height for given atmospheric conditions [6]–[8]. Enabled by structural approximation of turbine rotors, e.g. the actuator disk model (ADM) [9], more sophisticated variants were developed that observe conservation principles for mass and momentum [10], [11]. Recent efforts have also been made to include 3D effects caused when turbines are yawed via curled wake profiles [12]. The predictions of such static models of the velocity field typically depend on a set of parameters that can be tuned to match field measurements or LES data, e.g., [13]–[15]. Nevertheless, in the absence of a dynamical model for the background turbulence, wake recovery is often under-predicted and interactions with the atmospheric boundary layer cannot be accounted for autonomously.

To overcome the shortcomings of static models, contributions have been made to add a degree of dynamics or parametric stochasticity to analytical models, e.g., the stochastic ADM model [16] or the dynamic extension of the Park model [17]. In addition to such models, the linearized Navier-Stokes (NS) equations were combined with vortex cylinder theory to provide a physics-based alternative for dynamical modeling of wind farm flows [18]. However, in the absence of nonlinear terms, such linearized models lack the quantitative accuracy in predicting flow statistics or quantities of interest for control design, e.g., thrust force or power generation at turbines. To address this problem, we build on the stochastic dynamical modeling framework of [19]–[21] to augment the predictions of low-fidelity analytical models with the fluctuating velocity field obtained via stochastically forced linear models that are trained to match SCADA measurements or LES-generated data.

A. Challenge and contribution

The energy extraction process that is based on the actuator disc concept [9, Chapter 3] yields the following expressions for the thrust force exerted on the rotor disk of a turbine and the power extracted by the rotor:

$$F \;=\; \frac{1}{2}\,\rho\, A\, C_T\, \mathbf{u}^2, \qquad P \;=\; \frac{1}{2}\,\rho\, A\, C_P\, \mathbf{u}^3. \tag{1}$$

Here, F is the thrust force, P is the power, ρ is the air density, A is the area of the rotor disk, C_T is the thrust coefficient, C_P is the power coefficient, and $\mathbf{u}$ is the effective disk-averaged

The presenting author is grateful to the Center for Wind Energy at UT Dallas for providing travel support.

Aditya H. Bhatt and A. Zare are with the Department of Mechanical Engineering, University of Texas at Dallas, Richardson, TX 75080, USA. E-mails: {aditya.bhatt, armin.zare}@utdallas.edu.

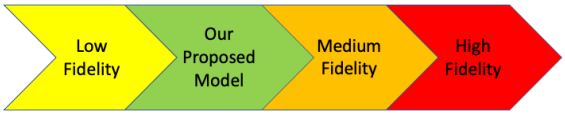

Fig. 1. Our proposed modeling approach uses data to augment the predictive capability of low-fidelity engineering models using a stochastic dynamical representation of atmospheric turbulence whereby improved predictions of power and thrust force can be achieved.

velocity on the rotor disk. The power and thrust coefficients can be defined as functions of the axial induction factor a that is used to quantify the induced flow at the actuator disk due to the pressure variation over the turbine:

$$C_T \;=\; 4a\,(1\,-\,a)\,, \quad C_P \;=\; 4a\,(1\,-\,a)^2\,.$$

Low-fidelity analytical models such as the Frandsen [10] or the Jensen-Park [6], [7] models predict the wind velocity in the wake of turbines under steady atmospheric conditions. Such models neglect the time-varying near-field turbulence behind the wind turbine and are often combined with linear wake superposition laws providing an over-simplified static prediction of the wind velocity. In the absence of a turbulence model that can induce mixing in the turbine wakes, velocity deficits are typically over-predicted by such models leading to inaccurate predictions of quantities of interest for wind farm control, i.e., the load and power corresponding to each turbine. In contrast, medium fidelity models, e.g., those that are based on the Reynolds-averaged NS equations, are not prone to such issues as they capture the 3D dynamic variation of the velocity field and introduce turbulence models that enable wake recovery [22], [23].

In this paper, we seek linear dynamical models of the velocity field in a wind farm that compensate the shortcomings of low-fidelity models by accounting for second-order statistics of the velocity field that are pertinent in the prediction of thrust force and power using Eq. (1). To this end, we adopt the stochastic dynamical modeling framework of [19]–[21] to model the effect of atmospheric turbulence as an input stochastic forcing. The power spectral density of the stochastic input is prescribed by inverse problems that are formulated to improve predictions of the thrust force and power. The data in our inverse problems are informed by SCADA measurements or LES. Our approach offers a data-driven dynamical enhancement to low-fidelity models that improves their predictive capability without adding to their dimensional complexity giving rise to linear time-invariant (LTI) models that are well-suited for analysis and synthesis using tools from modern robust control; see Fig. 1.

B. Paper outline

In Sec. II, we formulate a problem to address the challenge of matching thrust force and power generation by accounting for the dynamics of velocity fluctuations around static flow fields. In Sec. III, we summarize the stochastic modeling framework that we use to match the thrust force and power at various turbines. In Sec. IV, we provide a model for the turbulent velocity field at the hub height of a wind farm using the stochastically forced linearized NS equations. In Sec. V, we apply our approach to the problem of matching LES-informed quantities of interest in a 4×1 array of turbines. We conclude with remarks and future directions in Sec. VI.

II. Problem formulation

The wind velocity field $\mathbf{u}$ can be decomposed into the sum of a time-averaged mean $\bar{\mathbf{u}}$ and zero-mean fluctuations $\mathbf{v}$ as

$$\mathbf{u} \;=\; \bar{\mathbf{u}} + \mathbf{v}, \quad \bar{\mathbf{u}} \;=\; \mathbf{E}\,[\mathbf{u}]\,, \quad \mathbf{E}\,[\mathbf{v}] \;=\; 0 \tag{2}$$

where $\mathbf{E}\,[\cdot]$ denotes the time-average operator, e.g.,

$$\mathbf{E}\,[\mathbf{u}(\mathbf{x},t)] \;=\; \lim_{T\to\infty} \frac{1}{T} \int_0^T \mathbf{u}(\mathbf{x}, t\,+\,\tau)\,\mathrm{d}\tau.$$

Here, $\mathbf{x}$ denotes the spatial coordinates and t is time. The velocity fluctuations $\mathbf{v}$, which we will use to capture the effect of atmospheric turbulence on the wake model, are assumed to be stochastic Gaussian processes. Substituting this decomposition into Eqs. (1) yields

$$F \;=\; \frac{1}{2}\rho\, A\, C_T\, (\bar{\mathbf{u}}^2 \,+\, \overline{\mathbf{v}^2}), \quad P \;=\; \frac{1}{2}\rho\, A\, C_P\, (\bar{\mathbf{u}}^3 \,+\, 3\,\bar{\mathbf{u}}\,\overline{\mathbf{v}^2}) \tag{3}$$

where, the overline denotes an average over the surface of the rotor disk $\mathcal{S}$, i.e.,

$$\overline{\mathbf{v}^2} \;=\; \int_{\mathcal{S}} \mathbf{E}\left[\mathbf{v}(\mathbf{x},t)^2\right] \mathrm{d}\mathbf{x} \tag{4}$$

and the properties of the fluctuation field $\mathbf{v}$, namely its zero mean (cf. Eq. (2)) and skewness (due to its Gaussian distribution) have been used to eliminate certain terms. Based on Eq. (3), the scalar quantities that we obtain for the thrust force and power of each turbine will not only depend on the mean disk-averaged velocity $\bar{\mathbf{u}}$ at the turbine, but also on the disk-averaged second-order statistics of a fluctuation field $\mathbf{v}$. While analytical models provide a static prediction of the effective velocity in the wind farm (similar to $\bar{\mathbf{u}}$), the fluctuation field $\mathbf{v}$ provides an additional degree-of-freedom whose second-order statistics can be modeled to improve predictions of the thrust force and power.

Given a set of available thrust force $\{\bar{F}_i\}$ and power $\{\bar{P}_i\}$ measurements for turbines across a wind farm, the dynamics of $\mathbf{v}$ can be sought to augment the predictions of static analytical models by providing the necessary surface integrals $\overline{\mathbf{v}^2}$ to better predict the available data (cf. Eq. (3)). Together with the *prior* low-fidelity model that predicts $\bar{\mathbf{u}}$, the dynamical model identified for $\mathbf{v}$ can provide a class of low-complexity models that are more accurate in predicting quantities that depend on turbulent flow statistics. To this end, we adopt a stochastic dynamical modeling approach that is based on stochastically forced LTI approximations of complex dynamical systems [19]–[21]. Specifically, we assume the dynamics of velocity fluctuations that complement the static predictions of $\bar{\mathbf{u}}$ to follow the state-space representation

$$\begin{aligned} \boldsymbol{\psi}_t(\mathbf{x},t) \;&=\; \mathbf{A}\,\boldsymbol{\psi}(\mathbf{x},t) \;+\; \mathbf{B}\,\mathbf{d}(\mathbf{x},t) \\ \mathbf{v}(\mathbf{x},t) \;&=\; \mathbf{C}\,\boldsymbol{\psi}(\mathbf{x},t). \end{aligned} \tag{5}$$

Here, $\boldsymbol{\psi}$ is the state, $\mathbf{d}$ is a stationary zero-mean stochastic process, $\mathbf{A}$ is the dynamic generator that represents a prior

dynamical representation for the wake dynamics, $\mathbf{B}$ is the input operator that is used to introduce the input $\mathbf{d}$ into the dynamics, and $\mathbf{C}$ is an output operator that relates the state $\boldsymbol{\psi}$ to the output velocity field $\mathbf{v}$. In Sec. V, we use the stochastically forced linearized NS equations as a physics-based dynamical model for the evolution of fluctuations $\mathbf{v}$. We note, however, that alternative linear models, which may result from application specific assumptions/simplifications, or data-driven methods such as dynamic mode decomposition [24]–[27] may also provide viable starting points.

A finite-dimensional approximation of the operators in Eq. (5) over the spatial dimensions yields

$$\begin{aligned} \dot{\boldsymbol{\psi}}(t) &= A\,\boldsymbol{\psi}(t) + B\,\mathbf{d}(t) \\ \mathbf{v}(t) &= C\,\boldsymbol{\psi}(t) \end{aligned} \tag{6}$$

where $\boldsymbol{\psi}(t)$, $\mathbf{v}(t)$, $\mathbf{d}(t)$, A, B, and C are real-valued vectors and matrices of appropriate dimensions. We next summarize our approach for the stochastic realization of process $\mathbf{d}$ that induces a statistical response $\mathbf{v}$ that achieves consistency with LES in predicting power and thrust force measurements.

III. Stochastic dynamical modeling of partially available second-order statistics

We assume knowledge of a set of measurements for the thrust force and power of turbines in a wind farm. This information, together with an initial prediction of the effective mean velocity $\bar{\mathbf{u}}$ from a low-fidelity static model can be used to identify second-order statistics of the effective fluctuating component that are needed to achieve the best possible prediction of the available data with linear Gaussian model (6). In this section, we provide background material on structural constraints on state covariances of LTI systems and formulate covariance completion problems that identify the statistics of forcing $\mathbf{d}$ and enable its stochastic realization.

A. Second-order statistics

For system (6) with Hurwitz A and controllable pair (A, B), matrix X qualifies as the steady-state covariance matrix of the state vector, i.e., $X = \lim_{t\to\infty} \mathbf{E}\,[\boldsymbol{\psi}(t)\,\boldsymbol{\psi}^*(t)]$, if and only if the Lyapunov-like equation

$$A\,X + X\,A^* = -B\,H^* - H\,B^* \tag{7}$$

is solvable for the matrix H [28], [29]. Here, $*$ denotes the complex conjugate transpose. The matrix H quantifies the cross-correlation between the input and the state in model (6) [20, Appendix B]:

$$H := \lim_{t\to\infty} \mathbf{E}\,[\boldsymbol{\psi}(t)\mathbf{d}^*(t)] + \frac{1}{2}B\,\Omega.$$

When the stochastic input $\mathbf{d}$ is zero-mean and white-in-time with covariance Ω, $H = (1/2)B\,\Omega$, which reduces Eq. (7) to the standard algebraic Lyapunov equation

$$A\,X + X\,A^* = -B\,\Omega B^*.$$

The one-point velocity correlations that are integrated to obtain $\overline{\mathbf{v}^2}$ (Eq. (4)) represent entries of the output covariance matrix $\Phi = \lim_{t\to\infty} \mathbf{E}\,[\mathbf{v}(t)\,\mathbf{v}^*(t)]$, which is linearly related to the state covariance matrix via $\Phi = CXC^*$.

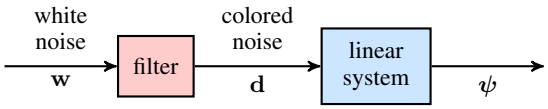

Fig. 2. A cascade connection of an LTI system with a linear filter that is designed to account for the sampled steady-state covariance matrix X.

B. Covariance completion

Given partially known entries of Φ corresponding to the deficit in thrust force and power predictions relative to LES-generated data, we seek an input matrix B and statistics of forcing $\mathbf{d}$ that are consistent with the hypothesis that the required statistics in $\mathbf{v}$ are generated by model (6) with known generator A. Moreover, it is also important to restrict the complexity of the forcing model, which we quantify using the number of degrees of freedom that are directly influenced by the stochastic forcing, i.e., the number of input channels or $\mathrm{rank}(B)$. To these ends, we follow [19]–[21] in solving the structured covariance completion problem:

$$\begin{aligned} \underset{X,\,Z}{\text{minimize}} \quad & -\log\det(X) + \gamma\,\|Z\|_* \\ \text{subject to} \quad & A\,X + X\,A^* + Z = 0 \\ & (CXC^*)\circ E - G = 0 \end{aligned} \tag{8}$$

which penalizes a composite objective subject to two linear constraints. Here, matrices A, C, E, and G are problem data, and Hermitian matrices X and Z are optimization variables. Entries of G represent partially available second-order statistics of the output $\mathbf{v}$, the symbol $\circ$ denotes elementwise matrix multiplication, and E is the structural identity matrix:

$$E_{ij} = \begin{cases} 1, & \text{if } G_{ij} \text{ is available} \\ 0, & \text{if } G_{ij} \text{ is unavailable.} \end{cases}$$

The objective function provides a trade-off between the solution to a maximum-entropy problem and the complexity of the forcing model; the logarithmic barrier ensures the positive definiteness of matrix X and the nuclear norm regularizer, which is weighted by the parameter $\gamma > 0$, is used as a proxy for the rank function (see, e.g., [30], [31]). The rank of matrix Z bounds the number of independent input channels or columns in matrix B; for details see [19]. Convex optimization (8) can be cast as a semidefinite program and solved efficiently using standard solvers [32]–[34] for small-size problems. In [19], [35], customized algorithms have been developed to deal with larger problems. The solution to problem (8) can be used to construct a low-pass filter that generates the suitable colored-in-time forcing $\mathbf{d}$ in Eqs. (6) (Fig. 2); see [19] for additional details.

IV. Linearized Navier-Stokes equations

In this section, we specialize our dynamical modeling approach to the stochastically forced linearized NS equations around a static velocity profile $\bar{\mathbf{u}}$ that is generated by a low-fidelity model. For simplicity, we restrict mathematical

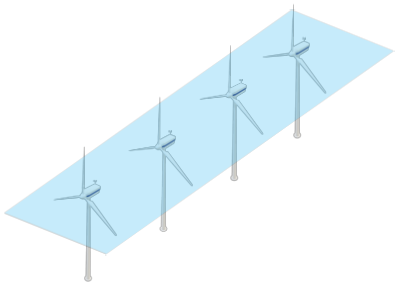

Fig. 3. A cascade of 4 wind turbines where turbine 1 is the most upstream.

developments to the 2D domain at hub height (Fig. 3) and assume all turbines to be facing the wind, i.e., 0° yaw angle relative to the free-stream velocity U_∞. As a result, the average velocity field $\bar{\mathbf{u}}$ will only have a streamwise component in the direction of the free-stream wind. We note that our approach is not limited to 2D models and that more complicated farm arrangements involving various pitch and yaw angles can also be accounted for.

The linearized NS equations around $\bar{\mathbf{u}}$ are given by

$$\begin{aligned} \mathbf{v}_t \;&=\; -\left(\nabla\cdot\mathbf{v}\right)\bar{\mathbf{u}} - \left(\nabla\cdot\bar{\mathbf{u}}\right)\mathbf{v} - \nabla p + \frac{1}{Re}\Delta\mathbf{v} - K^{-1}\mathbf{v} \\ 0 \;&=\; \nabla\cdot\mathbf{v} \end{aligned} \tag{9}$$

where $\mathbf{v} = [\,u\;\; w\,]^T$ consists of the fluctuating velocity field in the streamwise (u) and spanwise (w) directions, p is the vector of pressure fluctuations, ∇ is the gradient operator, $\Delta = \nabla\cdot\nabla$ is the Laplacian, and the Reynolds number $Re = U_\infty d_0/\nu$ is defined in terms of the rotor diameter d_0, free-stream velocity U_∞, and kinematic viscosity ν. All variables in Eqs. (9) have been non-dimensionalized: length by d_0, velocity by U_∞, time by d_0/U_∞, and pressure by ρU_∞^2.

In Eqs. (9), we have captured the effect of turbine rotors and nacelles on the velocity field using the volume penalization technique proposed by Khadra et al. [36]. This method avoids the implementation of boundary conditions in complex geometries by modeling the effect of solid obstructions of the flow as a spatially varying permeability function K that influences the governing equations as a static feedback term. Within the fluid, the penalization resulting from K should have no influence on the flow, i.e., $K \to \infty$, yielding back the original linearized NS dynamics for $\mathbf{v}$. On the other hand, within solid structures, the function K should force the velocity field to zero, i.e., $K \to 0$. To capture the spatial region that is influence by the presence of the turbines we use the smooth filter function

$$\begin{aligned} K^{-1}(x,z) = \frac{c}{\pi^2}\big[\arctan(a(x-x_1)) - \arctan(a(x-x_2))\big] \\ \times\,\big[\arctan(a(z-z_1)) - \arctan(a(z-z_2))\big] \end{aligned} \tag{10}$$

where $x_{1,2}$ and $z_{1,2}$ determine the spatial extent of the rotors in the horizontal plane and parameters a and c determine the magnitude and slope of the function.

By expressing the velocity fluctuations in terms of the stream function ϕ, i.e., $u = \partial_z\,\phi$ and $w = -\partial_x\,\phi$, pressure can be removed form the Eqs. (9) bringing the linearized dynamics (9) into the form:

$$\begin{aligned} \phi_t \;=\; -\,\Delta^{-1}\Big(\,&\bar{\mathbf{u}}\,\partial_x\nabla \;+\; \bar{\mathbf{u}}_x\,\nabla \;+\; \bar{\mathbf{u}}_{xz}\,\partial_z \;-\; \bar{\mathbf{u}}_{zz}\,\partial_x \\ &-\frac{1}{Re}\Delta^2 \;+\; K^{-1}\Delta \;+\; (\nabla K^{-1})\cdot\nabla\Big)\,\phi \end{aligned} \tag{11}$$

where $\bar{\mathbf{u}}_x$ and $\bar{\mathbf{u}}_z$ denote the derivatives of $\bar{\mathbf{u}}$ with respect to the x and z. Homogeneous Dirichlet and Neumann boundary conditions are implemented at the boundaries of the 2D domain, i.e.,

$$\begin{aligned} \phi(x(0),z) \;&=\; 0, \quad \phi(x(L_x),z) \;=\; 0 \\ \phi(x,z(0)) \;&=\; 0, \quad \phi(x,z(L_z)) \;=\; 0 \\ \phi_x(x(0),z) \;&=\; 0, \quad \phi_x(x(L_x),z) \;=\; 0 \\ \phi_z(x,z(0)) \;&=\; 0, \quad \phi_z(x,z(L_z)) \;=\; 0 \end{aligned}$$

where L_x and L_z denote the length of the 2D domain in the streamwise and spanwise directions, respectively.

V. Numerical Experiment

In this section, we provide a data-enhanced dynamical model for the turbulent velocity field at hub height for a cascade of 4 identical turbines (Fig. 3). Similar to Sec. IV, we assume all turbines to be facing the wind, i.e., 0° yaw angle relative to the free-stream velocity U_∞. The thrust force and power at each turbine ($\{\bar{F}_i\}$ and $\{\bar{P}_i\}$), which constitute the data in our problem, are generated by an LES code [4], [5] that solves the filtered NS equations when the turbine blades are modeled using the actuator line model [37].

We consider a 2D computational domain of size $L_x \times L_z = 22 \times 5$; $x \in [\,0,\;\; 22\,]$ and $z \in [\,-2.5,\;\; 2.5\,]$ with turbines located at $x = \{3, 8, 13, 18\}$ and $z = 0$. As there is no cross-wind, the time-averaged velocity field will only consist of a streamwise component. The analytical wake model proposed by [11],

$$\begin{aligned} \bar{\mathbf{u}}(x,z) \;=\; U_\infty - U_\infty\left(1 - \sqrt{1 - \frac{C_T}{8\left(k^\star x/d_0 + 0.25\sqrt{\beta}\right)^2}}\right) \\ \times\,\exp\left(-\frac{1}{2\left(k^\star x/d_0 + 0.25\sqrt{\beta}\right)^2}\left(\frac{z}{d_0}\right)^2\right) \end{aligned} \tag{12}$$

is used together with a linear superposition law for velocity deficits to provide the static hub-height velocity field $\bar{\mathbf{u}}$ for this cascade of turbines (Fig. 4). Here, the diameter of turbines is set to $d_0 = 1$, the wake growth rate of $k^\star = 0.03$ is chosen in accordance with earlier studies (e.g., [15]), and $\beta = (1 + \sqrt{1 - C_T}/(2\sqrt{(1 - C_T)}))$. Choices of $C_P = 0.4858$ and $C_T = 0.7871$ correspond to the maximum power generated by a 5MW NREL turbine [38] using an LES code that leverages blade momentum element theory [4], [5].

As shown in Fig. 6, the velocity field predicted by the low-fidelity analytical model (12) yields quantitatively poor predictions of the thrust force and power generation at the turbines (cf. Eq. (1)). It is also evident that the monotonically decreasing $\bar{\mathbf{u}}$ fails to capture the increase in the thrust force and power after the second turbine. We thus seek the statistics

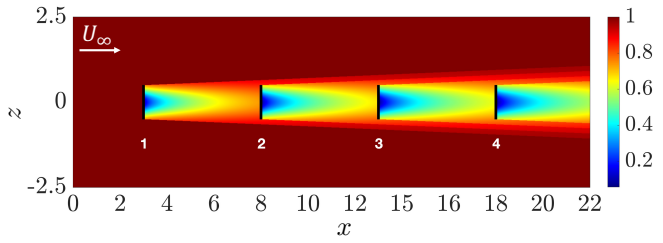

Fig. 4. The streamwise and spanwise dependence of $\bar{\mathbf{u}}(x, z)$ generated by Eq. (12) over the 2D computational domain at hub height. The thick black lines mark the location of the turbine rotors with diameter $d_0 = 1$.

of velocity fluctuations $\mathbf{v}$ around $\bar{\mathbf{u}}$ to improve predictions of the low-fidelity model. To this end, we use the stochastically forced linearized NS equations described in Sec. IV and follow the stochastic modeling framework of Sec. III to improve predictions of power and thrust force over the farm.

The operators in the evolution form (6) corresponding to the stream function dynamics (11) are provided in the appendix. For discretization, we use a 4th-order central difference scheme with $N_x = 21$ and $N_z = 9$ collocation points in x and z, respectively, which renders the state $\phi \in \mathbb{R}^{189\times 1}$. In this experiment, $Re = 10^8$ and the resistance function K^{-1} used in the linearized equations for the 4×1 array of turbines is shown in Fig. 5.

Following Sec. III-B, we use the solution to problem (8) to identify the input matrix B and statistics of forcing $\mathbf{d}$ that allow us to match either the set of LES-generated thrust forces $\{\bar{F}_i\}$ or power $\{\bar{P}_i\}$ and predict the other. As shown in Fig. 6, our modeling approach provides the necessary dynamical perturbation to the linearized NS equations for matching the LES data (cf. Fig. 6(a,d)), and significantly improve predictions of quantities that are not assumed to be known (cf. Fig. 6(b,c)). We note that matching both $\{\bar{F}_i\}$ and $\{\bar{P}_i\}$ is not possible because of the limited degrees of freedom in Eqs. (3), but a least-squares balance in matching F and P can provide a reasonable simultaneous estimation of both quantities of interest; see Fig. 7.

VI. Concluding Remarks

We provide a wake modeling framework for improved predictive capability relative to conventional low-fidelity models. We particularly focus on the estimation of quantities that are pertinent to control, i.e., thrust forces and power generation. We use LES-generated measurements of thrust forces and/or power to identify stochastic realizations of forcing into linear approximations of the turbulent flow dynamics to achieve consistency in matching statistical quantities of interest. To demonstrate the utility of our approach, we use the stochastically forced linearized NS equations around a 2D static velocity profile of a wind farm consisting of a cascade of 4 turbines and show that stochastic modeling of input forcing allows us to significantly improve the predictions of low-fidelity analytical models. Our control-oriented models are: (1) physics-based; (2) linear; (3) dynamic; and (4) low complexity. The proposed framework allows for linearization around more complicated (potentially 3D) base flow profiles that can better represent turbine yawing or alternative turbine arrangements within a wind farm. Our ongoing efforts focus on extensions of the framework to the 3D domain to better capture vortex shedding effects from yawed turbines as well as exploring alternative covariance completion formulations [39], [40] that may provide useful information about critical directions that have maximal effect in bringing model (in our case the stochastically forced linearized NS) and statistics in agreement.

Acknowledgments

We thank Prof. M. Rotea for insightful discussions; and F. Bernardoni and Prof. S. Leonardi for providing the LES data used in the numerical experiment of Sec. V.

Appendix

The system matrices in Eqs. (6) are given as

$$A = -\Delta^{-1}\Big(\bar{\mathbf{u}}\,\partial_x\nabla + \bar{\mathbf{u}}_x\,\nabla + \bar{\mathbf{u}}_{xz}\,\partial_z - \bar{\mathbf{u}}_{zz}\,\partial_x - \frac{1}{Re}\Delta^2 + K^{-1}\Delta + (\nabla K^{-1})\cdot\nabla\Big)$$

$$B = \Delta^{-1}\begin{bmatrix}\partial_z & -\partial_x\end{bmatrix}; \quad C = \begin{bmatrix}\partial_z \\ -\partial_x\end{bmatrix}.$$

References

[1] P. Veers, K. Dykes, E. Lantz, S. Barth, C. L. Bottasso, O. Carlson, A. Clifton, J. Green, P. Green, H. Holttinen, *et al.*, "Grand challenges in the science of wind energy," *Science*, vol. 366, no. 6464, 2019.

[2] R. Barthelmie, S. T. Frandsen, K. Hansen, J. Schepers, K. Rados, W. Schlez, A. Neubert, L. E. Jensen, and S. Neckelmann, "Modelling the impact of wakes on power output at Nysted and Horns Rev," in *European Wind Energy Conference*, 2009, pp. 1–10.

[3] M. Churchfield, S. Lee, and P. Moriarty, "Overview of the simulator for wind farm application (sowfa)," *National Renewable Energy Laboratory*, 2012.

[4] C. Santoni, K. Carrasquillo, I. Arenas-Navarro, and S. Leonardi, "Effect of tower and nacelle on the flow past a wind turbine," *Wind Energy*, vol. 20, no. 12, pp. 1927–1939, 2017.

[5] C. Santoni, E. J. García-Cartagena, U. Ciri, L. Zhan, G. V. Iungo, and S. Leonardi, "One-way mesoscale-microscale coupling for simulating a wind farm in North Texas: Assessment against SCADA and LiDAR data," *Wind Energy*, vol. 23, no. 3, pp. 691–710, 2020.

[6] N. O. Jensen, "A note on wind generator interaction," 1983.

[7] I. Katic, J. Højstrup, and N. O. Jensen, "A simple model for cluster efficiency," in *European wind energy association conference and exhibition*, vol. 1, 1986, pp. 407–410.

[8] J. F. Ainslie, "Calculating the flowfield in the wake of wind turbines," *J. Wind Eng. Ind. Aerodyn.*, vol. 27, no. 1-3, pp. 213–224, 1988.

[9] T. Burton, N. Jenkins, D. Sharpe, and E. Bossanyi, *Wind energy handbook*. John Wiley & Sons, 2011.

[10] S. Frandsen, R. Barthelmie, S. Pryor, O. Rathmann, S. Larsen, J. Højstrup, and M. Thøgersen, "Analytical modelling of wind speed deficit in large offshore wind farms," *Wind Energy: An International Journal for Progress and Applications in Wind Power Conversion Technology*, vol. 9, no. 1-2, pp. 39–53, 2006.

[11] M. Bastankhah and F. Porté-Agel, "A new analytical model for wind-turbine wakes," *Renewable energy*, vol. 70, pp. 116–123, 2014.

[12] L. A. Martínez-Tossas, J. Annoni, P. A. Fleming, and M. J. Churchfield, "The aerodynamics of the curled wake: a simplified model in view of flow control," *Wind Energy Science*, vol. 4, no. 1, pp. 127–138, 2019.

[13] L. Wang, A. C. Tan, M. Cholette, and Y. Gu, "Comparison of the effectiveness of analytical wake models for wind farm with constant and variable hub heights," *Energy Conversion and Management*, vol. 124, pp. 189–202, 2016.

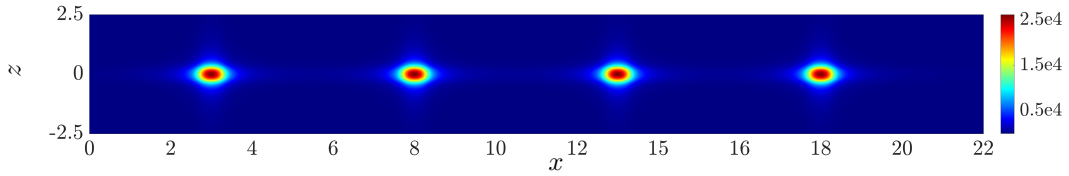

Fig. 5. Streamwise and spanwise dependence of the resistance function $K^{-1}(x, z)$ based on Eq. (10)).

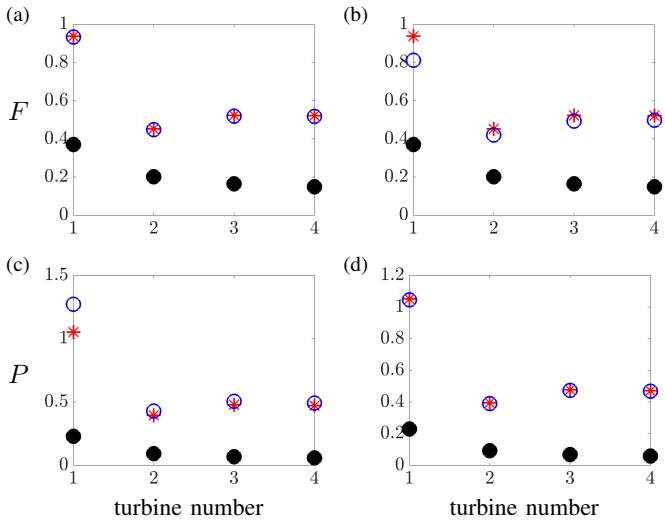

Fig. 6. Estimated thrust force (a,b) and power generation (c,d) over the 4×1 cascade of wind turbines. (a,c) LES-generated thrust forces $\{\bar{F}_i\}$ are used to train our model and power is predicted; (b,d) LES-generated power measurements $\{\bar{P}_i\}$ are used to train the our model and thrust forces are predicted. LES data ($*$); results of analytical model (12) from [11] ($\bullet$); and results of our data-enhanced stochastic dynamical model ($\bigcirc$).

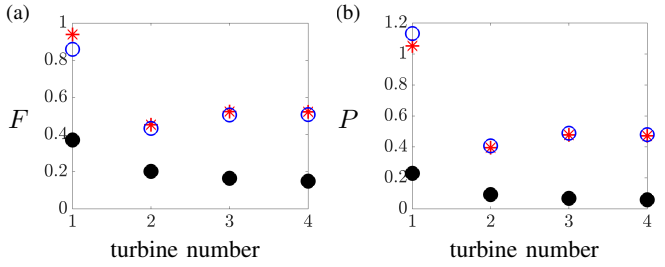

Fig. 7. Estimated thrust force (a) and power generation (b) over the wind turbines when the statistics of fluctuations $\mathbf{v}^2$ are found by establishing a least-squares balance in matching LES-generated thrust force $\{\bar{F}_i\}$ and power measurements $\{\bar{P}_i\}$. LES data ($*$); results of analytical model (12) from [11] ($\bullet$); and results of our data-enhanced dynamical model ($\bigcirc$).

[14] F. Campagnolo, A. Molder, J. Schreiber, and C. Bottasso, "Comparison of analytical wake models with wind tunnel data," in *Journal of Physics: Conference Series*, vol. 1256, no. 1. IOP Publishing, 2019, p. 012006.

[15] L. Zhan, S. Letizia, and G. Iungo, "Optimal tuning of engineering wake models through lidar measurements," *Wind Energy Science*, vol. 5, no. 4, pp. 1601–1622, 2020.

[16] Y. Guo, M. Rotea, and T. Summers, "Stochastic dynamic programming for wind farm power maximization," in *2020 American Control Conference (ACC)*. IEEE, 2020, pp. 4824–4829.

[17] J. Annoni, K. Howard, P. Seiler, and M. Guala, "An experimental investigation on the effect of individual turbine control on wind farm dynamics," *Wind Energy*, vol. 19, no. 8, pp. 1453–1467, 2016.

[18] M. Soleimanzadeh, R. Wisniewski, and A. Brand, "State-space representation of the wind flow model in wind farms," *Wind Energy*, vol. 17, no. 4, pp. 627–639, 2014.

[19] A. Zare, Y. Chen, M. R. Jovanovic, and T. T. Georgiou, "Low-complexity modeling of partially available second-order statistics: theory and an efficient matrix completion algorithm," *IEEE Trans. Automat. Control*, vol. 62, no. 3, pp. 1368–1383, March 2017.

[20] A. Zare, M. R. Jovanovic, and T. T. Georgiou, "Colour of turbulence," *J. Fluid Mech.*, vol. 812, pp. 636–680, February 2017.

[21] A. Zare, T. T. Georgiou, and M. R. Jovanovic, "Stochastic dynamical modeling of turbulent flows," *Annu. Rev. Control Robot. Auton. Syst.*, vol. 3, pp. 195–219, May 2020.

[22] G. V. Iungo, F. Viola, U. Ciri, S. Leonardi, and M. Rotea, "Reduced order model for optimization of power production from a wind farm," in *34th Wind Energy Symposium*, 2016, p. 2200.

[23] S. Boersma, B. Doekemeijer, M. Vali, J. Meyers, and J.-W. van Wingerden, "A control-oriented dynamic wind farm model: WFSim," *Wind Energy Sci.*, vol. 3, no. 1, pp. 75–95, 2018.

[24] P. J. Schmid, "Dynamic mode decomposition of numerical and experimental data," *J. Fluid Mech.*, vol. 656, pp. 5–28, 2010.

[25] M. R. Jovanovic, P. J. Schmid, and J. W. Nichols, "Sparsity-promoting dynamic mode decomposition," *Phys. Fluids*, vol. 26, no. 2, p. 024103 (22 pages), February 2014.

[26] J. R. Annoni, J. Nichols, and P. J. Seiler, "Wind farm modeling and control using dynamic mode decomposition," in *34th Wind Energy Symposium*, 2016, p. 2201.

[27] P. J. Schmid, "Dynamic mode decomposition and its variants," *Annu. Rev. Fluid Mech.*, vol. 54, p. 2022, 2021.

[28] T. T. Georgiou, "The structure of state covariances and its relation to the power spectrum of the input," *IEEE Trans. Autom. Control*, vol. 47, no. 7, pp. 1056–1066, 2002.

[29] T. T. Georgiou, "Spectral analysis based on the state covariance: the maximum entropy spectrum and linear fractional parametrization," *IEEE Trans. Autom. Control*, vol. 47, no. 11, pp. 1811–1823, 2002.

[30] M. Fazel, "Matrix rank minimization with applications," Ph.D. dissertation, Stanford University, 2002.

[31] B. Recht, M. Fazel, and P. A. Parrilo, "Guaranteed minimum-rank solutions of linear matrix equations via nuclear norm minimization," *SIAM Rev.*, vol. 52, no. 3, pp. 471–501, 2010.

[32] K.-C. Toh, M. J. Todd, and R. H. Tütüncü, "SDPT3-a MATLAB software package for semidefinite programming, version 1.3," *Optim. Methods Softw.*, vol. 11, no. 1-4, pp. 545–581, 1999.

[33] M. Grant and S. Boyd, "CVX: Matlab software for disciplined convex programming, version 2.1," http://cvxr.com/cvx, Mar. 2014.

[34] S. Boyd and L. Vandenberghe, *Convex optimization*. Cambridge University Press, 2004.

[35] A. Zare, M. R. Jovanovic, and T. T. Georgiou, "Alternating direction optimization algorithms for covariance completion problems," in *Proceedings of the 2015 American Control Conference*, Chicago, IL, 2015, pp. 515–520.

[36] K. Khadra, P. Angot, S. Parneix, and J. Caltagirone, "Fictitious domain approach for numerical modelling of Navier-Stokes equations," *Int. J. Numer. Methods Fluids*, vol. 34, no. 8, pp. 651–684, 2000.

[37] J. N. Sorensen and W. Z. Shen, "Numerical modeling of wind turbine wakes," *J. Fluids Eng.*, vol. 124, no. 2, pp. 393–399, 2002.

[38] J. Jonkman, S. Butterfield, W. Musia, and G. Scott, "Definition of a 5-mw reference wind turbine for offshore system development," National Renewable Energy Lab.(NREL), Golden, CO (United States), Tech. Rep., 2009.

[39] A. Zare, M. R. Jovanovic, and T. T. Georgiou, "Perturbation of system dynamics and the covariance completion problem," in *Proceedings of the 55th IEEE Conference on Decision and Control*, 2016, pp. 7036–7041.

[40] A. Zare, H. Mohammadi, N. K. Dhingra, T. T. Georgiou, and M. R. Jovanović, "Proximal algorithms for large-scale statistical modeling and sensor/actuator selection," *IEEE Trans. Automat. Control*, vol. 65, no. 8, pp. 3441–3456, August 2020.